PNAS RESEARCH ARTICLE | MICROBIOLOGY OPEN ACCESS

Lenacapavir disrupts HIV-1 core integrity while stabilizing the capsid lattice

Chenglei Li[a,1], Ryan C. Burdick[a,1], Rokeya Siddiqui[a], Sanath Kumar Janaka[a], Ru-ching Hsia[b], Wei-Shau Hu[c], and Vinay K. Pathak[a,2]

Affiliations are included on p. 11.

Edited by Stephen Goff, Columbia University Medical Center, New York, NY; received October 7, 2024; accepted February 19, 2025

Lenacapavir (GS-6207; LEN) is a potent HIV-1 capsid inhibitor approved for treating multidrug-resistant infection. LEN binds to a hydrophobic pocket between neighboring capsid (CA) proteins in hexamers and stabilizes the capsid lattice, but its effect on HIV-1 capsids is not fully understood. Here, we labeled HIV-1 capsids with green fluorescent protein fused to CA (GFP-CA) or a fluid-phase GFP content marker (cmGFP) to assess LEN's impact on HIV-1 capsids. HIV-1 cores labeled with GFP-CA, but not cmGFP, could be immunostained with an anti-GFP antibody and were less sensitive to the capsid-binding host restriction factor MX2, demonstrating that GFP-CA is incorporated into the capsid lattice and is a marker for capsid lattice stability, whereas cmGFP is an indicator of core integrity. LEN treatment of isolated HIV-1 cores resulted in a dose-dependent loss of cmGFP signal while preserving the GFP-CA signal, indicating that LEN disrupts core integrity but stabilizes the capsid lattice. In contrast, capsid inhibitor PF-3450074 (PF74) induced loss of core integrity and the capsid lattice. Electron microscopy of LEN- or PF74-treated viral cores revealed frequent breakage at the narrow end of the capsid and other morphological changes. Our results suggest that LEN treatment does not prevent nuclear envelope docking but inhibits nuclear import of cores with or without loss of core integrity. In contrast, PF74 treatment blocks nuclear import by inhibiting the nuclear envelope docking of viral cores, highlighting their different mechanisms of nuclear import inhibition.

HIV-1 | capsid | core integrity | lenacapavir | GS-6207

Significance

Capsid inhibitor lenacapavir (GS-6207; LEN) binds to HIV-1 cores and potently blocks virus replication. We evaluated LEN's effects on HIV-1 capsids using two labeling methods: GFP content marker (cmGFP) to measure capsid integrity and GFP-tagged capsid (GFP-CA) to track capsid lattice stability. Our in vitro assays with isolated HIV-1 cores and cell-based assays demonstrated that LEN disrupts viral core integrity and stabilizes the capsid lattice. Viral cores in LEN-treated cells docked at the nuclear envelope but failed to enter the nucleus, suggesting that LEN-induced alterations in the capsid lattice impair nuclear import. In contrast, the less potent capsid inhibitor PF-3450074 blocks nuclear import by preventing viral core docking with the nuclear envelope, highlighting their different mechanisms of nuclear import inhibition.

HIV type 1 (HIV-1) is a retrovirus that infects and destroys certain $CD4^+$ immune cells and is the causative agent of AIDS. After fusion of the viral and cell membranes, the HIV-1 capsid containing the viral genome and replicative enzymes enters the cytoplasm of the infected cell (reviewed in ref. 1). The cone-shaped capsid, composed of approximately 250 hexamers and exactly 12 pentamers of the capsid protein (CA) (2, 3), must disassemble (uncoat) so that the newly synthesized double-stranded DNA copy of the viral genome can integrate into the host genome. We previously developed methods to study HIV-1 uncoating, including direct labeling of CA with green fluorescent protein (GFP-CA) and tracking the rare viral cores that lead to productive infection (4). Our results showed that the viral cores uncoat in the nucleus shortly before integration and near the integration site. In addition, we labeled viral cores with a GFP content marker (cmGFP) that is released upon loss of viral core integrity (5–7) and demonstrated that viral cores remain intact through nuclear import and until just before capsid disassembly (5). Since the size of a single cmGFP molecule (28 kD) is comparable to that of a single CA protein (24 kD), small holes or ruptures in the capsid lattice are likely to result in the loss of the cmGFP marker. Therefore, cmGFP serves as a sensitive indicator of capsid lattice disruption; here, we refer to cores with the cmGFP marker as "intact" or "cores with integrity" and cores without the cmGFP marker as "broken" or "cores with integrity loss." Consistent with our findings, other studies have shown that the HIV-1 capsid is intact after nuclear entry and sensitive to capsid inhibitor PF-3450074 (PF74) (8), an intact capsid is necessary for reverse transcription (9), and that reverse transcription is completed in the nucleus (4, 8, 10, 11). Recent cryogenic electron tomography studies have also shown that conical-shaped capsids enter the nuclei of infected cells (12–14).

Current antiretroviral therapy (ART) regimens can suppress viral replication in people living with HIV-1 to undetectable levels and prevent transmission. However, ART leads to the emergence of drug resistance, compromising the effectiveness of treatments (15). The development of new classes of antiretroviral drugs that target different aspects of HIV-1 replication is needed to effectively control virus replication of drug-resistant variants. Due to its finely regulated and critical roles throughout the HIV-1 life cycle, the HIV-1 capsid has recently emerged as a promising target for antiviral drugs. PF74 binds

Author contributions: C.L., R.C.B., W.-S.H., and V.K.P. designed research; C.L., R.C.B., R.S., and R.-c.H. performed research; S.K.J. contributed new reagents/analytic tools; C.L., R.C.B., R.S., R.-c.H., W.-S.H., and V.K.P. analyzed data; and C.L., R.C.B., W.-S.H., and V.K.P. wrote the paper.

The authors declare no competing interest.

This article is a PNAS Direct Submission.

[1]C.L. and R.C.B. contributed equally to this work.

[2]To whom correspondence may be addressed. Email: pathakv@mail.nih.gov.

This article contains supporting information online at https://www.pnas.org/lookup/suppl/doi:10.1073/pnas.2420497122/-/DCSupplemental.

Published April 1, 2025.

a hydrophobic pocket composed of neighboring CA monomers within a CA hexamer (16, 17) and inhibits virus replication with a 50% effective concentration (EC_{50}) of 0.56 μM (17). The hydrophobic binding site, often referred to as the phenylalanine-glycine (FG)-binding pocket, binds FG-motifs present in host factors involved in the early stage of HIV-1 replication, including NUP153, cleavage, and polyadenylation specificity factor 6 (CPSF6), and SEC24C (4, 16, 18–25). Although PF74 was not considered a viable lead compound due to its low metabolic stability, several novel PF74-like molecules with improved potency and potentially higher metabolic stability have been developed (26). GS-6207 (lenacapavir; LEN) is a first-in-class, ultrapotent (EC_{50} of ~23 pM), and long-acting HIV-1 capsid inhibitor that recently gained approval from both the European Union and the US Food and Drug Administration for the treatment of multidrug-resistant HIV-1 infection (27). Structural studies indicate that LEN binds the FG-binding pocket and stabilizes the capsid lattice (23, 27).

Both PF74 and LEN can inhibit multiple steps in the early stage of infection, including reverse transcription, nuclear import, and integration, likely by directly altering capsid stability (17, 23, 27) and interfering with host factor binding (23, 28, 29). However, few studies have directly examined the effects of these inhibitors on HIV-1 capsids in infected cells. Fate-of-capsid assays revealed that LEN stabilizes the HIV-1 capsid in infected cells and prevents viral core uncoating and infection (30, 31). However, fate-of-capsid assays cannot distinguish between intact or broken capsids. The number of cytoplasmic viral cores labeled by the indirect HIV-1 capsid marker cyclophilin A (CypA)-DsRed (32) increased with LEN treatment (23), but it was not determined whether viral cores were intact or broken or whether the increased number of cytoplasmic cores was due to decreased nuclear import or increased viral core stability. In contrast, PF74 treatment resulted in a rapid disappearance of most nuclear viral cores (4, 33) and reduced the amounts of pelletable capsid in fate-of-capsid assays (16, 30, 34), suggesting that PF74 induces capsid disassembly in infected cells. Interestingly, treating infected cells with PF74 (10 μM) or LEN (10 nM) after synthesis of reverse transcription products resulted in a rapid loss of viral DNA, suggesting that both PF74 and LEN disrupt viral cores, allowing host nucleases to access viral DNA (35). Thus, the effects of LEN in infected cells—specifically whether it increases capsid stability and inhibits uncoating, or whether it induces capsid disassembly—are not well understood.

Methods that can accurately quantify the level of CA associated with individual viral cores are needed to understand the effect of capsid inhibitors on viral cores in infected cells. Recent studies using amber codon suppression to directly label CA with noncanonical amino acids conjugated to organic fluorophores concluded that intact or mostly intact HIV-1 capsids enter the nucleus (13, 33). While these findings are consistent with our studies using GFP-CA-labeled viral cores (4), a recent study suggested that GFP-tagged CA is associated with the viral ribonucleoprotein complex (vRNP) inside the capsid and is not incorporated into the capsid lattice (36).

Here, we utilized in vitro assays with isolated viral cores and cell-based assays to examine the localization of GFP-CA and cmGFP in HIV-1 capsids. We observed that contrary to the previous report (36), GFP-CA is incorporated into the capsid lattice and serves as a marker for capsid disassembly. We also observed that cmGFP is passively trapped inside capsids during virion maturation and serves as a marker for core integrity. We then leveraged these different capsid labeling strategies to determine the effect of LEN and PF74 on HIV-1 capsids using in vitro and cell-based assays. Overall, we found that LEN disrupts viral core integrity while stabilizing the capsid lattice both in vitro and in vivo, whereas PF74 disrupts viral core integrity as well as destabilizes the capsid lattice, providing insights into the effect of LEN on HIV-1 capsids in infected cells. Furthermore, we found that LEN does not block viral core docking at the nuclear envelope but inhibits the translocation of the viral cores into the nucleus, whereas PF74 inhibits nuclear import by blocking nuclear envelope docking.

Results

Isolation of Viral Cores Labeled with GFP-CA or cmGFP. Viruses labeled with cmGFP or GFP-CA were produced and visualized by fluorescence microscopy using previously described methods (Fig. 1*A*) (4, 5). For cmGFP labeling, GFP was flanked by protease cleavage sites and inserted between matrix (MA) and CA. Approximately 20% of the GFP released from the Gag precursor during virus maturation incorporates into the mature capsid and is released upon loss of viral core integrity (5). This GFP serves as a viral core content marker (cmGFP) that can be used to distinguish between intact viral cores and viral cores that have lost their integrity. For GFP-CA labeling, the protease cleavage site between GFP and CA was mutated to release a GFP-CA fusion protein from the Gag precursor during virus maturation. Because some of the GFP-CA is expected to be incorporated into the CA lattice of mature capsids, this label can be used to visualize the viral core directly. To generate infectious virus particles that can be visualized by fluorescence microscopy, HIV-1 plasmids expressing cmGFP or GFP-CA and HIV-1 plasmids expressing wild-type (WT) Gag were cotransfected into 293T producer cells at 1:2 (cmGFP:WT) and 1:10 (GFP-CA:WT) ratios. Western blot analysis of the virion lysates indicated that cmGFP and GFP-CA were detected and were efficiently cleaved from the p55Gag-GFP precursor whereas GFP or GFP-CA were not detected in the unlabeled (WT) virus (Fig. 1*B*).

To isolate viral cores, virions were loaded onto a sucrose gradient containing 200 μM inositol hexakisphosphate (IP6) and subjected to ultracentrifugation (Fig. 1*C*). Western blot analysis indicated that mature viral cores sedimented predominantly to fractions 19–20, as indicated by the presence of p24, and that GFP-CA and cmGFP were also detected in these fractions (Fig. 1 *D* and *E*). The presence of unprocessed Gag (p55 and p55-GFP) in fractions 22–23 indicated that immature virus particles sedimented predominantly to the bottom of the gradient. The GFP signals from mature viral cores and immature viral particles (fractions 19–23) were visualized by fluorescence microscopy (Fig. 1 *F* and *G*). Although fluorescent particles were detected in all fractions, the median GFP intensity of mature viral cores labeled with GFP-CA (hereafter referred to as GFP-CA viral cores) was ~2.5- to 5.0-fold lower than the median GFP intensity of immature viral particles labeled with GFP-CA (hereafter referred to as GFP-CA immature particles) (Fig. 1*F*). Although HIV-1 virions typically contain ~5,000 Gag monomers, mature capsids are composed of only ~1,500 CA subunits assembled into a hexagonal lattice (37). The reduced level of GFP-CA associated with mature capsids compared to immature viral particles is consistent with the idea that a small proportion of the total GFP-CA in virions, like CA, assembles into the mature capsid (4). The ~2.4- to 5.0-fold higher GFP levels associated with GFP-CA immature particles can be explained by the greater number of GFP molecules in the form of unprocessed p55-GFP that are expected to be present in immature viral particles compared to mature capsids. The median GFP intensity of mature viral cores labeled with cmGFP

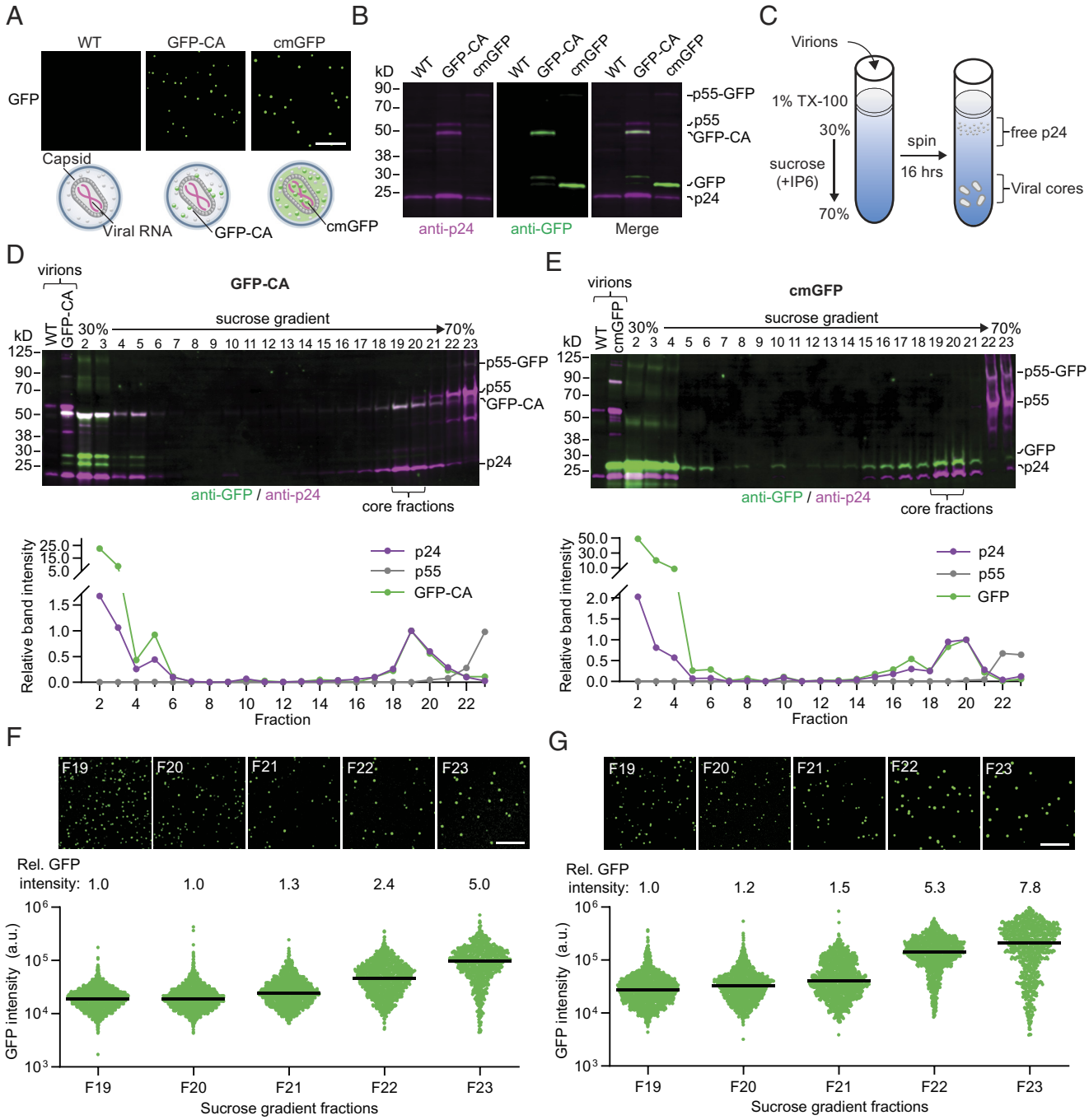

Fig. 1. Intact HIV-1 cores labeled with GFP-CA or cmGFP isolated by sucrose density gradient fractionation. (*A*) Representative images and schematics of unlabeled HIV-1 virions (WT) or virions labeled with GFP-CA or cmGFP. HIV-1 plasmids expressing cmGFP or GFP-CA and HIV-1 plasmids expressing WT Gag were cotransfected into 293T producer cells at 1:10 (GFP-CA:WT) and 1:2 (cmGFP:WT) ratios. (*B*) Western blot of unlabeled (WT), GFP-CA labeled, and cmGFP labeled viruses probed with anti-p24 and anti-GFP antibodies. (*C*) Schematic of sucrose gradient fractionation protocol used to isolate viral cores. (*D* and *E*) Western blots of 23 fractions obtained from sucrose gradient fractionation of detergent-treated HIV-1 virions labeled with GFP-CA (*D*) or cmGFP (*E*) and probed with anti-p24 and anti-GFP antibodies. Virion lysates were loaded as controls. Mature viral cores containing p24 sediment predominantly to fractions 19 and 20. Quantitation of the western blots in (*D*) shows relative band intensities of processed GFP-CA and p24 (fraction 19 set to 1) and p55 (shown relative to p24 in fraction 19). Quantitation of the western blots in (*E*) shows relative band intensities of processed GFP and p24 (fraction 20 set to 1) and p55 (shown relative to p24 in fraction 20). (*F* and *G*) Representative images of GFP fluorescent particles obtained from sucrose gradient fractions 19 through 23 for HIV-1 particles labeled with GFP-CA (*F*) or cmGFP (*G*). GFP fluorescence intensities of particles from each fraction are shown below the corresponding representative images; black lines indicate median. The number of particles analyzed for each fraction ranged from 995 to 6,284 for (*F*) and 882 to 2,569 for (*G*). (Scale bars, 10 μm.)

(hereafter referred to as cmGFP viral cores) was 5.3- to 7.8-fold lower than the median GFP intensity of immature particles (Fig. 1*G*). These results are consistent with previous studies showing that most of the cmGFP, which is between the viral membrane and the capsid, is lost immediately upon viral fusion (5, 6, 38). Overall, these findings indicate that mature viral cores labeled with GFP-CA or cmGFP can be isolated from virions using sucrose gradient sedimentation and visualized using fluorescence microscopy.

HIV-1 Mature Cores Labeled with GFP-CA, but Not cmGFP, Are Immunostained with Anti-GFP Antibody. The accessibility of GFP-CA and cmGFP to an anti-GFP antibody labeled with Alexa Fluor 647 (AF647) was determined using isolated viral cores.

Most of the GFP-CA particles (~92%) from the mature core fractions could be efficiently detected with the anti-GFP(AF647) antibody whereas few of the cmGFP particles (~7%) from the mature core fractions were anti-GFP(AF647)$^+$ (Fig. 2 *A* and *B*). The median GFP intensity of the cmGFP$^+$/anti-GFP(AF647) negative viral cores was ~2.0-fold higher than that of GFP-CA$^+$/anti-GFP(AF647)$^+$ viral cores, indicating the low detection efficiency of anti-GFP(AF647) antibody for the cmGFP viral cores was not a result of lower GFP levels (Fig. 2*C*). The GFP intensities of the few GFP-CA viral cores (8%) that were not detected by the anti-GFP antibody were only slightly lower (~90%) than the GFP intensities of the viral cores that were anti-GFP(AF647)$^+$; this suggests that under the conditions of our assay, efficiency of capsid detection by the anti-GFP(AF647) antibody is ~92%, even though the viral cores that were anti-GFP(AF647) negative had similar, but slightly lower level of GFP-CA in the capsid (Fig. 2*C*). The AF647 intensity of the GFP-CA viral cores positively correlated with the GFP intensity (*SI Appendix*, Fig. S1). Interestingly, the median GFP intensity of the few cmGFP particles from the mature core fraction that were detected with the anti-GFP(AF647) antibody was ~3-fold higher than the median GFP intensity of the anti-GFP(AF647) negative particles (Fig. 2*C*) and similar to the median GFP intensity of immature particles (Fig. 1*G*; fractions 22–23), suggesting these anti-GFP(AF647)$^+$ signals were immature capsid particles.

Detection with an AF647-labeled anti-MA antibody, which is expected to only bind immature particles containing p55 Gag and not isolated mature cores, was used to determine the percentage of immature particles that cosediment in the mature core fractions. An average of ~5 to 6% of the GFP-CA and cmGFP particles were detected with the anti-MA(AF647) antibody (Fig. 2 *D* and *E*). The median GFP intensity of the particles that were detected with the anti-MA(AF647) antibody was 3.5- to 4.5-fold higher than the median GFP intensity of particles that were not detected with the anti-MA(AF647) antibody (Fig. 2*F*) and similar to the median GFP intensity of immature particles (Fig. 1 *F* and *G*; fractions 22–23). As expected, the immature viral particles (fraction 22) were efficiently detected by the anti-GFP(AF647) and anti-MA(AF647) antibodies (*SI Appendix*, Fig. S2). Overall, these results indicate the GFP-CA protein associated with mature viral cores, but not cmGFP associated with mature viral cores, is on the outside of mature viral cores and is accessible to the anti-GFP(AF647) antibody. Additionally, these results indicate that the fractions containing mostly mature cmGFP viral cores (fractions 19–20) also contain a small number of immature viral particles that can be detected with the anti-GFP(AF647) antibody. The results also show that the high GFP intensity associated with immature viral cores can be used to distinguish between mature viral cores and immature viral particles.

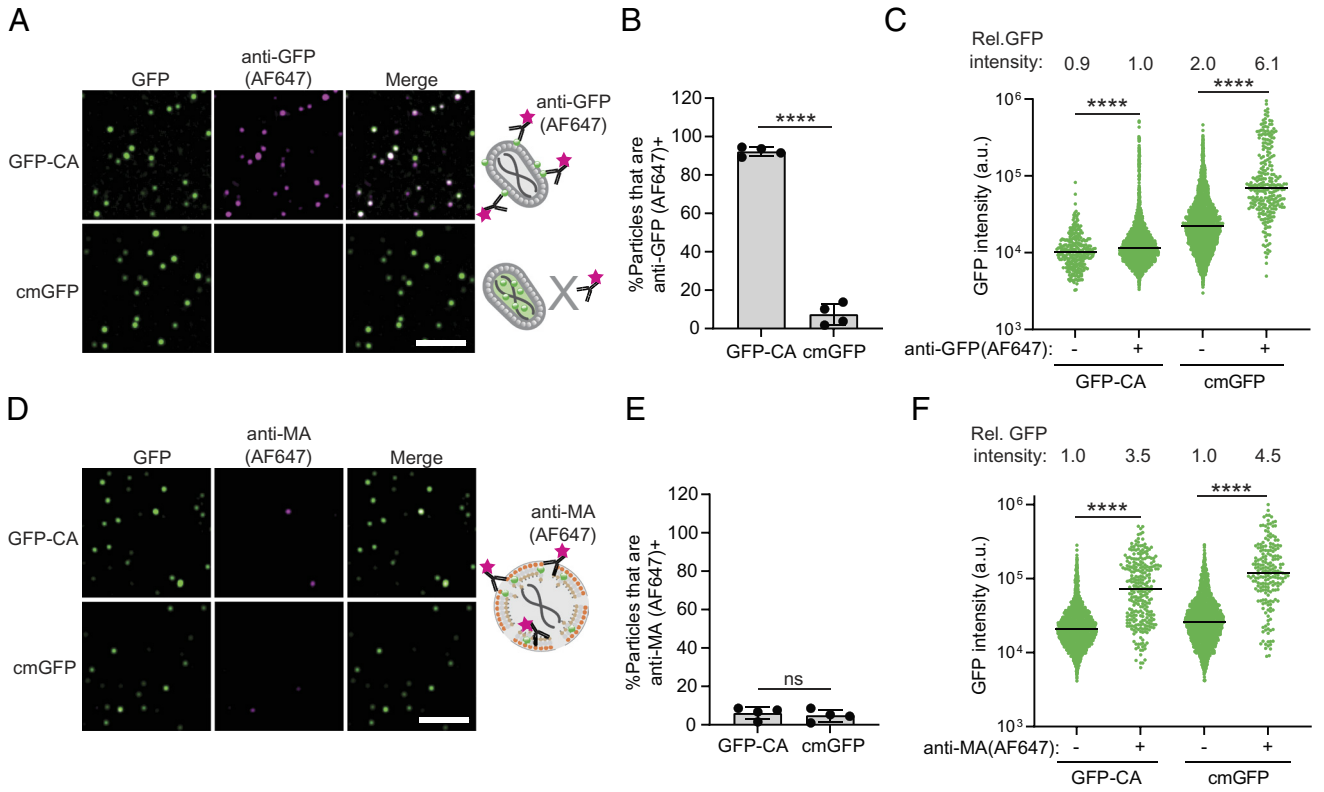

Fig. 2. Mature HIV-1 cores labeled with GFP-CA, but not cmGFP, are efficiently detected with anti-GFP antibody. (*A*) Representative images (*Left*) and schematic (*Right*) of mature HIV-1 cores labeled with GFP-CA or cmGFP (green) that were immunostained with Alexa Fluor 647 (AF647)-conjugated anti-GFP antibody (magenta). (*B*) The percentage of GFP-CA- or cmGFP particles that were AF647 positive after incubation with anti-GFP(AF647) antibody. (*C*) GFP fluorescence intensities were measured for GFP-CA particles that were either AF647 negative (291) or AF647 positive (5,466) after staining with anti-GFP(AF647) antibody and for cmGFP particles that were either AF647 negative (5,989) or AF647 positive (256) after staining with anti-GFP(AF647) antibody. (*C*) Same particles as in (*B*); lines are median. (*D*) Representative images (*Left*) and schematic (*Right*) of HIV-1 cores labeled with GFP-CA or cmGFP that were immunostained with AF647-conjugated anti-MA antibody. (*E*) The percentage of GFP-CA- or cmGFP particles that were AF647 positive after incubation with anti-MA(AF647) antibody. (*F*) GFP fluorescence intensities were measured for GFP-CA particles that were either AF647 negative (4,479) or AF647 positive (270) after staining with anti-MA(AF647) antibody and for cmGFP particles that were either AF647 negative (4,874) or AF647 positive (200) after staining with anti-MA(AF647) antibody. Same particles as in (*E*); black lines indicate median. For (*B*) and (*E*), data are mean ± SD from four independent experiments; *P* values are from Welch's *t* test. For (*C*) and (*F*), *P* values are from the Mann–Whitney test. ****$P < 0.0001$; ns, not significant ($P > 0.05$). (Scale bar, 10 μm.)

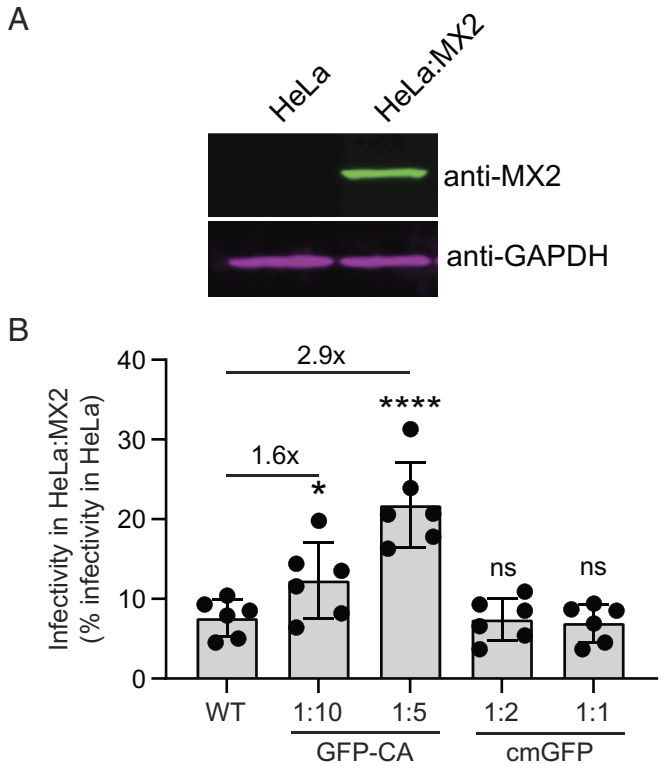

Fig. 3. Effect of GFP-CA and cmGFP on sensitivity to MX2 restriction. (*A*) Western blot of HeLa and HeLa:MX2 cells with anti-MX2 and anti-GAPDH antibodies. (*B*) Infectivity of unlabeled virions (WT), virions labeled with GFP-CA:WT at 1:10 and 1:5 ratios, and virions labeled with cmGFP:WT at 1:2 and 1:1 ratios in HeLa:MX2 cells. Infectivity is shown as % infectivity in plain HeLa cells for each virus. Data are mean ± SD from six independent experiments. *P* values are from Welch's *t* test. **P* < 0.05; *****P* < 0.0001, ns, not significant (*P* > 0.05).

GFP-CA Incorporation Into the Capsid Lattice Reduces Sensitivity to MX2 Restriction. Next, we determined whether GFP-CA incorporation into the capsid lattice alters the sensitivity to MX2, a host restriction factor that binds a negatively charged pocket at the interface of three CA hexamers on the surface of the HIV-1 capsid and inhibits nuclear import (39–41). Viruses were labeled with increasing amounts of GFP-CA or cmGFP by cotransfection of HIV-1 plasmids expressing GFP-CA or cmGFP and HIV-1 plasmid expressing WT Gag at different ratios (1:10 and 1:5 for GFP-CA:WT and 1:2 and 1:1 for cmGFP:WT). The infectivities of unlabeled (WT) viruses and viruses labeled with cmGFP in HeLa cells that do not express MX2 were similar (*SI Appendix*, Fig. S3). In contrast, the infectivities of GFP-CA viruses were ~73% (1:10) and ~39% (1:5) of the WT virus (*SI Appendix*, Fig. S3). Next, infectivity was measured in a HeLa cell line that expresses MX2 (Fig. 3*A*). The infectivities of WT virus and cmGFP virus were significantly lower in MX2-expressing cells relative to their infectivity in control cells (~7 to 8%; Fig. 3*B*), and similar to the level of inhibition observed in previous studies (40, 41). However, the infectivity of GFP-CA virus in MX2-expressing cells relative to control cells was 1.6-fold (1:10 ratio) and 2.9-fold (1:5 ratio) higher than the relative infectivity of WT virus in MX2-expressing cells (Fig. 3*B*), indicating that a higher number of GFP-CA viral cores escaped restriction by MX2 compared to unlabeled or cmGFP viral cores. These results are consistent with the observation that GFP-CA is incorporated into the capsid lattice and that GFP is facing outward, potentially interfering with MX2 binding or the formation of cytoplasmic biomolecular condensates (42). Overall, these results and the results showing that GFP-CA viral cores, but not cmGFP viral cores, are efficiently detected by anti-GFP(AF647) antibodies constitute strong evidence that GFP-CA is incorporated into the capsid lattice and is on the outside of the capsid and cmGFP is inside the viral cores. Therefore, GFP-CA serves as a marker for capsid lattice stability whereas cmGFP serves as a marker for viral core integrity. Cores that retain the GFP-CA marker for a longer or shorter time than WT cores are referred to as cores with "increased stability" or "decreased stability," respectively.

LEN Disrupts the Integrity of Isolated Mature Viral Cores. Before testing the effect of capsid inhibitors on isolated mature viral cores, we first determined the half-maximal effective concentration (EC_{50}) for LEN and PF74 using unlabeled, GFP-CA, and cmGFP viruses. We observed similar LEN and PF74 EC_{50} values for the three viruses (~0.04 nM and ~0.1 μM, respectively; *SI Appendix*, Fig. S4), indicating that the different labeling methods did not affect sensitivity to LEN or PF74. Next, we utilized isolated GFP-CA and cmGFP viral cores to determine the effect of LEN on the stability of the capsid lattice and viral core integrity. GFP-CA or cmGFP viral cores were centrifuged onto 8-well chamber slides and incubated for 20 min at 37 °C in a buffer containing 200 μM IP6 with or without LEN (Fig. 4*A*). The viral cores were imaged before and after treatment and the number of particles per field was quantified (Fig. 4 *B* and *C*). There was a modest decrease in the number of GFP-CA (~33%) and cmGFP (~16%) viral cores in the absence of LEN, indicating that some of the viral cores disassembled and became undetectable during the 20-min incubation. However, treatment of GFP-CA viral cores with increasing amounts of LEN (1, 10, and 100 nM) led to a dose-dependent increase in the number of GFP-CA viral cores up to the number of GFP-CA viral cores that were detected before the 20-min incubation (Fig. 4*C*). These results suggested that LEN treatment prevented the disassembly of GFP-CA viral cores during the 20-min incubation. Additionally, a modest decrease was observed in the median GFP intensity of GFP-CA viral cores treated with LEN compared to untreated GFP-CA viral cores (3%, 13%, and 14% for 1 nM, 10 nM, and 100 nM LEN, respectively; Fig. 4*D*). The reduction in GFP intensity suggested that while LEN stabilized the capsid lattice and prevented the disappearance of the GFP-CA viral cores, a small portion of the capsid lattice was still lost. In contrast to GFP-CA viral cores, treatment of cmGFP viral cores with increasing amounts of LEN led to a significant dose-dependent decrease in the number of cmGFP viral cores (Fig. 4*C*). The median GFP intensity of the few cmGFP particles that were detected after treatment with 100 nM LEN was significantly higher than the median GFP intensity of mature cores (Fig. 4*E*) and similar to the intensity of immature viral particles (Fig. 1*G*; fractions 22–23 and Fig. 2*F*), indicating these were likely LEN-insensitive immature viral particles. The LEN-mediated increase in the number of GFP-CA viral cores and decrease in the number of cmGFP viral cores indicate that LEN disrupts viral core integrity while stabilizing the capsid lattice (Fig. 4*C*).

Next, GFP-CA and cmGFP viral cores were incubated with 10 μM PF74, a concentration that led to the rapid disassembly of most (~86%) nuclear GFP-CA viral cores (4). Unlike LEN, treatment of isolated viral cores with 10 μM PF74 for 20 min led to a ~40% decrease in the number of observable GFP-CA viral cores (Fig. 4 *F* and *G*). A large decrease (~34%) in the median GFP intensity compared to that of untreated GFP-CA viral cores was observed (Fig. 4*H*), suggesting that a large portion of the capsid lattice of the detectable viral cores was lost. Like LEN treatment, PF74 treatment resulted in a significant decrease (~92%) in the number of cmGFP viral cores compared to untreated cmGFP viral

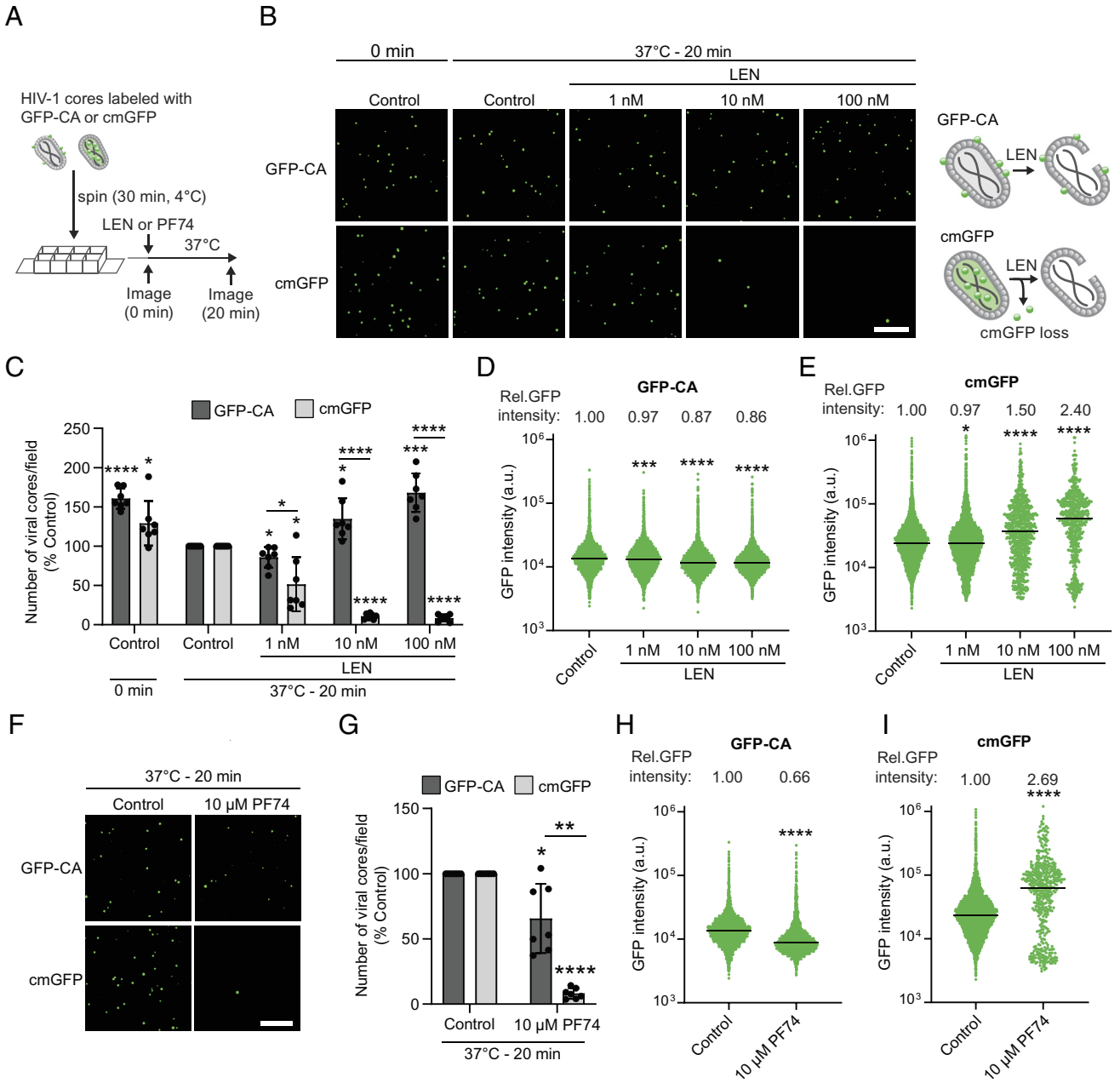

Fig. 4. LEN disrupts the integrity of isolated HIV-1 cores while stabilizing the capsid lattice. (*A*) Schematic of the protocol used to determine the effect of capsid inhibitors on mature HIV-1 cores labeled with GFP-CA or cmGFP. (*B*) Representative images of viral cores labeled with GFP-CA or cmGFP, with or without increasing concentrations of LEN. *Right*, schematics showing the effect of LEN-induced disruption of mature HIV-1 cores labeled with GFP-CA (*Top*) or cmGFP (*Bottom*). (*C*) Relative proportion of GFP-CA or cmGFP viral cores/field. Data are mean ± SD from seven independent experiments. (*D* and *E*) GFP fluorescence intensities were measured for GFP-CA (*D*) or cmGFP (*E*) particles; black lines indicate median. (*F*) Representative images of GFP-CA- or cmGFP viral cores, with or without 10 μM PF74. (*G*) Relative proportion of GFP-CA or cmGFP particles/field. Data are mean ± SD from seven independent experiments. (*H* and *I*) GFP fluorescence intensities were measured for GFP-CA (*H*) or cmGFP (*I*) particles; black lines indicate median. *P* values are from Welch's *t* test. ****$P < 0.0001$; ***$P < 0.001$; **$P < 0.01$; *$P < 0.05$. (Scale bars, 10 μm.)

cores (Fig. 4 *F* and *G*). The median GFP intensity of the few cmGFP particles that were detected after PF74 treatment was ~2.7-fold higher than that of mature cmGFP viral cores (Fig. 4*I*) and similar to the intensity of immature viral particles (Fig. 1*G*; fractions 22–23 and Fig. 2*F*), indicating that these were likely PF74-insensitive immature viral particles. These results indicate that PF74 binding to capsids results in the loss of viral core integrity and a significant loss of capsid lattice. Overall, these in vitro studies using isolated viral cores indicate that LEN or PF74 treatment leads to loss of viral core integrity. However, LEN stabilizes the capsid lattice whereas PF74 destabilizes the capsid lattice.

Structural Effect of LEN and PF74 on Viral Cores. To visualize the effect of LEN and PF74 on the structure of viral cores, we performed negative stain transmission electron microscopy (TEM) of isolated cmGFP viral cores treated without or with LEN (1, 10, and 100 nM) or PF74 (10 μM). We categorized the observed morphologies into four types: apparently intact, broken at the narrow end, broken (other), and aberrant (Fig. 5 *A* and *B* and Table 1). "Apparently intact" refers to capsids that appear intact, though we cannot rule out the possibility of small holes or ruptures that are not detectable. The terms "broken at the narrow end only" and "broken (other)" refer to visibly damaged capsids, with the former indicating breakage

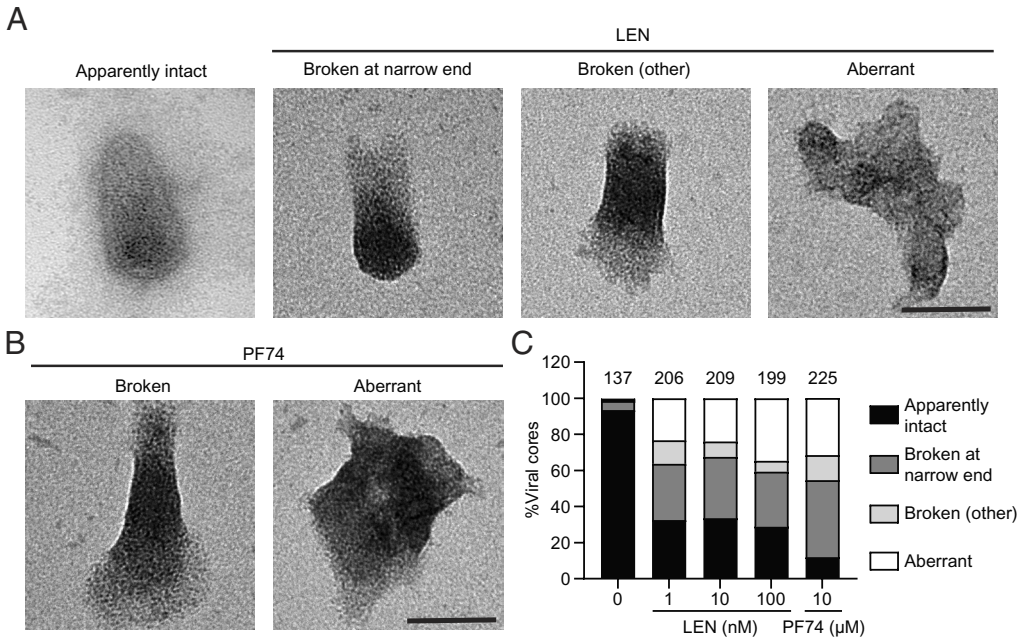

Fig. 5. Effect of LEN and PF74 on the morphology of HIV-1 capsids. (*A* and *B*) Representative negative stain transmission electron microscopy images of cmGFP HIV-1 cores treated with 100 nM LEN (*A*) or 10 μM PF74 (*B*) for 20 min. The capsid morphologies were classified into four categories: apparently intact, broken at the narrow end, broken (other), and aberrant. (*C*) Percentage of each core type for each condition. The number of HIV-1 cores analyzed for each condition ranged from 137 to 225 (shown above each bar). (Scale bars, 50 nm.)

exclusively at the narrow end (i.e., the tip of the conical-shaped shell) and the latter referring to breakage elsewhere on the capsid, either alone or in combination with damage at the narrow end. "Aberrant" refers to capsids that no longer resemble the classical conical shape. In untreated samples, most (~94%) viral cores were apparently intact (Fig. 5*C*). LEN treatment dramatically increased the percentage of viral cores that were broken (ranging from 36 to 44%) or exhibited aberrant morphology (ranging from 23 to 35%) (Table 1). Notably, among the broken cores, the majority (ranging from 70 to 83%) appeared to only be broken at the narrow end. Similar to LEN treatment, PF74 treatment primarily resulted in broken viral cores (57%) or aberrant viral cores (32%), and approximately 76% of the broken cores appeared to be broken only at the narrow end. Comparable results were obtained with negative stain TEM of isolated GFP-CA viral cores treated with LEN or PF74 (*SI Appendix*, Fig. S5 and Table 1).

LEN Disrupts Core Integrity While Stabilizing the Capsid Lattice of Viral Cores in the Nuclei of Infected Cells. To determine the effect of LEN on nuclear viral cores, HeLa cells were infected with GFP-CA or cmGFP HIV-1 and treated with 4 nM LEN (100× EC_{50}) ~4 h postinfection, a time when many viral cores have entered the nucleus but have not uncoated (4), and the nuclear viral cores were tracked for 3 h using live-cell imaging. Although it is unlikely that nuclear HIV-1 cores will encounter LEN because even subnanomolar LEN inhibits nuclear import (23), examining the effect of LEN on nuclear viral cores, which are exclusively mature capsids (14) and exhibit little movement (4, 43), provides a valuable assay for evaluating LEN's effects on viral cores in vivo. In contrast, the cytoplasm contains mature and immature capsids as well as virions trapped in endosomes (13, 44) and exhibits much more dynamic movement (45), making it unsuitable for long-duration live-cell imaging assays.

Although most GFP-CA (~96%) and cmGFP viral cores (~94%) in untreated cells remained detectable until the end of the 3-h observation period (Fig. 6 *A* and *B*), LEN treatment led to the rapid disappearance of most cmGFP viral cores (94%; median time of disappearance = ~93 min), but very few GFP-CA viral cores disappeared (4%; Fig. 6 *B* and *C*). Consistent with our previous observation (4), most GFP-CA viral cores disappeared after treatment with 10 μM PF74 (100× EC_{50}) (97%; median time of disappearance = ~13 min; Fig. 6 *B* and *C*). All cmGFP

Table 1. Effect of LEN or PF74 on the morphology of HIV-1 capsids

Core	Treatment		Apparently intact (%)	Broken at the narrow end (%)	Broken (other) (%)	Aberrant (%)	Total
cmGFP	LEN (nM)	0	128 (93.4)	7 (5.1)	1 (0.7)	1 (0.7)	137
		1	67 (32.5)	64 (31.1)****	27 (13.1)	48 (23.3)	206
		10	70 (33.5)	71 (34.0)****	18 (8.6)	50 (23.9)	209
		100	58 (29.1)	60 (30.2)****	12 (6.0)	69 (34.7)	199
	PF74 (μM)	10	27 (12.0)	96 (42.7)****	31 (13.8)	71 (31.6)	225
GFP-CA	LEN (nM)	0	108 (90.8)	6 (5.0)	1 (0.8)	4 (3.4)	119
		1	74 (36.1)	64 (31.3)****	36 (17.6)	31 (15.1)	205
		10	73 (34.3)	64 (30.0)****	27 (12.7)	49 (23.0)	213
		100	54 (27.0)	51 (25.5)****	22 (11.0)	73 (36.5)	200
	PF74 (μM)	10	40 (18.0)	67 (30.2)****	32 (14.4)	83 (37.4)	222

****$P < 0.0001$ from Fisher's exact test comparison of the proportion of cmGFP or GFP-CA viral cores that are broken at the narrow end in the untreated control (0 LEN) with the proportions in the presence of LEN or PF74.

viral cores disappeared after 10 μM PF74 treatment at a similar time as GFP-CA viral cores (median time of disappearance = ~13 min; $P > 0.05$), indicating PF74-induced loss of viral core integrity and loss of the capsid lattice occurred at a similar time. Overall, these results suggest that LEN leads to loss of viral core integrity without inducing capsid disappearance whereas PF74 leads to loss of viral core integrity by increasing capsid disappearance. Interestingly, the kinetics of capsid breakage were significantly slower with LEN compared to PF74 (93 min vs. 13 min, respectively). To determine whether the kinetics of loss of capsid integrity is dependent on LEN concentration, we determined the effect treating nuclear viral cores with 100 nM LEN. The cmGFP viral cores disappeared with faster kinetics compared to 4 nM LEN (~4 min vs. ~93 min; *SI Appendix*, Fig. S6), indicating that the kinetics of capsid breakage is dependent upon LEN concentration. A large fraction (39%) of the GFP-CA viral cores disappeared after 100 nM LEN treatment, suggesting that, in contrast to the in vitro experiments, many nuclear viral cores lost enough capsid lattice to become undetectable.

LEN and PF74 Inhibit Nuclear Import of HIV-1 Cores by Different Mechanisms. We previously demonstrated that stable association of HIV-1 cores with the nuclear envelope and their subsequent nuclear import are prerequisites for productive infection (4, 5, 43). To better understand how LEN and PF74 inhibit HIV-1 replication, we investigated the effects of treating cells with different concentrations of LEN or PF74 (5X and 25X EC_{50}) at the time of infection on the ability of HIV-1 cores to associate with the nuclear envelope and enter the nucleus using live-cell imaging (Fig. 7*A*). In untreated cells, similar numbers of GFP-CA and cmGFP viral cores were observed at the nuclear envelope (Fig. 7*B*). Treatment of cells with either concentration of PF74 (0.5 and 2.5 μM), but not LEN (0.2 or 1.0 nM), resulted in a reduction in GFP-CA viral cores at the nuclear envelope (Fig. 7*B*), suggesting that PF74, but not LEN, inhibits viral core docking with the nuclear envelope. We previously showed that 2 μM PF74 was insufficient to disrupt viral core integrity (5), suggesting that the reduction in the number of nuclear envelope-associated viral cores in cells treated with 0.5 μM PF74, and likely 2.5 μM PF74, was not due to viral core disassembly and loss of detection. Notably, a higher proportion of intact viral cores at the nuclear envelope—determined by the ratio of cmGFP to GFP-CA cores—was observed in cells treated with 0.2 nM LEN compared to cells treated with 1.0 nM LEN (Fig. 7*C*). This suggests that 0.2 nM LEN is insufficient to disrupt viral core integrity and that viral cores disrupted by 1.0 nM LEN can still associate with the nuclear envelope. As expected, treatment with either concentration of LEN or PF74 strongly inhibited nuclear import of viral cores (Fig. 7*D*). Comparable numbers of GFP-CA and cmGFP cores were observed in the nucleus for all conditions, indicating that only intact viral cores successfully entered the nucleus (Fig. 7 *D* and *E*). Overall, these findings suggest that PF74 inhibits nuclear import by preventing capsid association with the nuclear envelope, whereas LEN blocks the translocation of capsids from the nuclear envelope to the nucleus. Moreover, treatment with

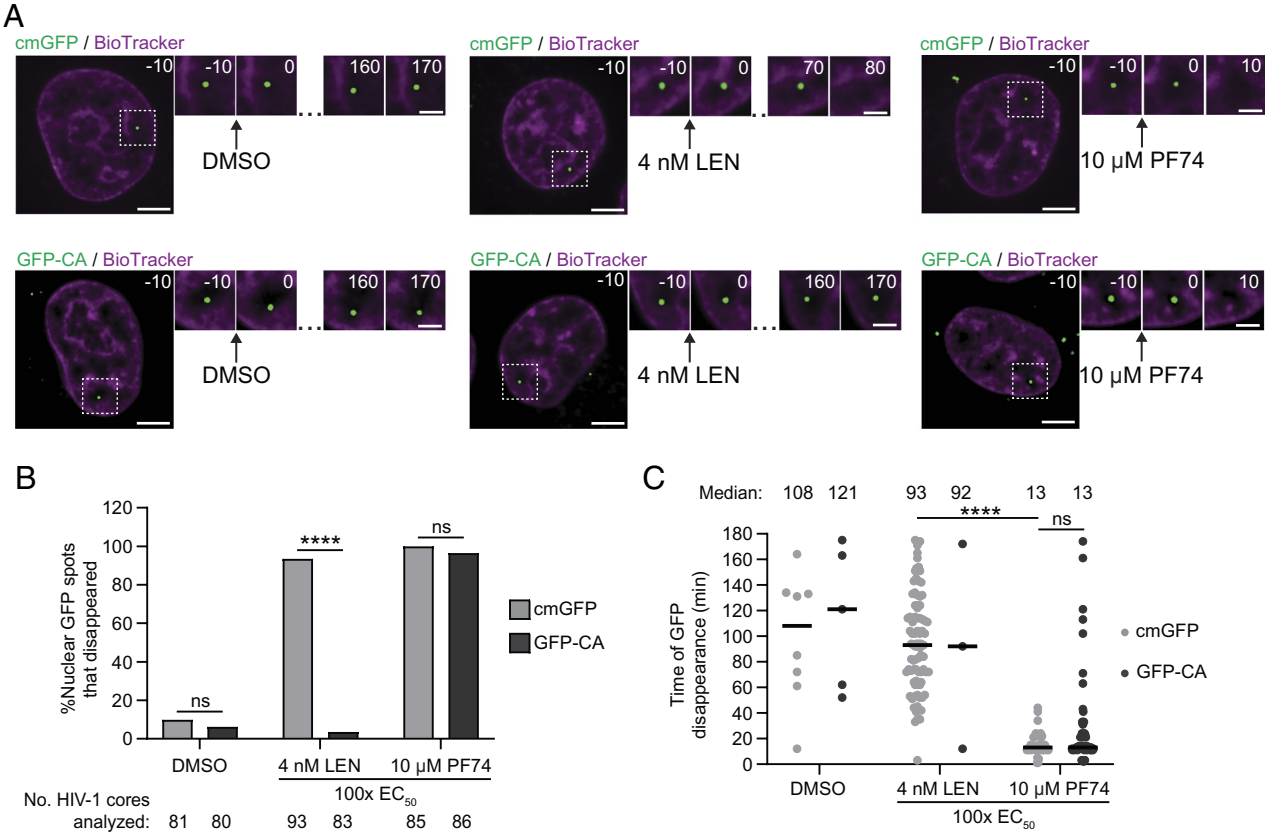

Fig. 6. LEN disrupts the integrity of nuclear HIV-1 capsids while stabilizing the capsid lattice. (*A*) Representative images of nuclear HIV-1 cores labeled with cmGFP (top row) or GFP-CA (bottom row) after treatment with DMSO, 4 nM LEN, or 10 μM PF74. HeLa cells were infected with HIV-1 labeled with cmGFP or GFP-CA, stained with BioTracker 650 Red Nuclear Dye (magenta), and imaged by confocal microscopy approximately 4 h after infection. Cells were treated with the indicated capsid inhibitor (or DMSO) after HIV-1 cores had entered the nucleus; the time (min) relative to capsid inhibitor addition is shown. (Scale bar, 5 μm; *Inset* scale bar, 2 μm.) (*B*) The percentage of nuclear HIV-1 cores that disappeared during the 3-h observation time with and without capsid inhibitor treatment. (*C*) The time (min) of GFP disappearance relative to capsid inhibitor addition. Thick black lines indicate median. For (*B*), *P* values are from Fisher's Exact Test. For (*C*), *P* values are from the Mann–Whitney test. ****$P < 0.0001$; ns, not significant ($P > 0.05$).

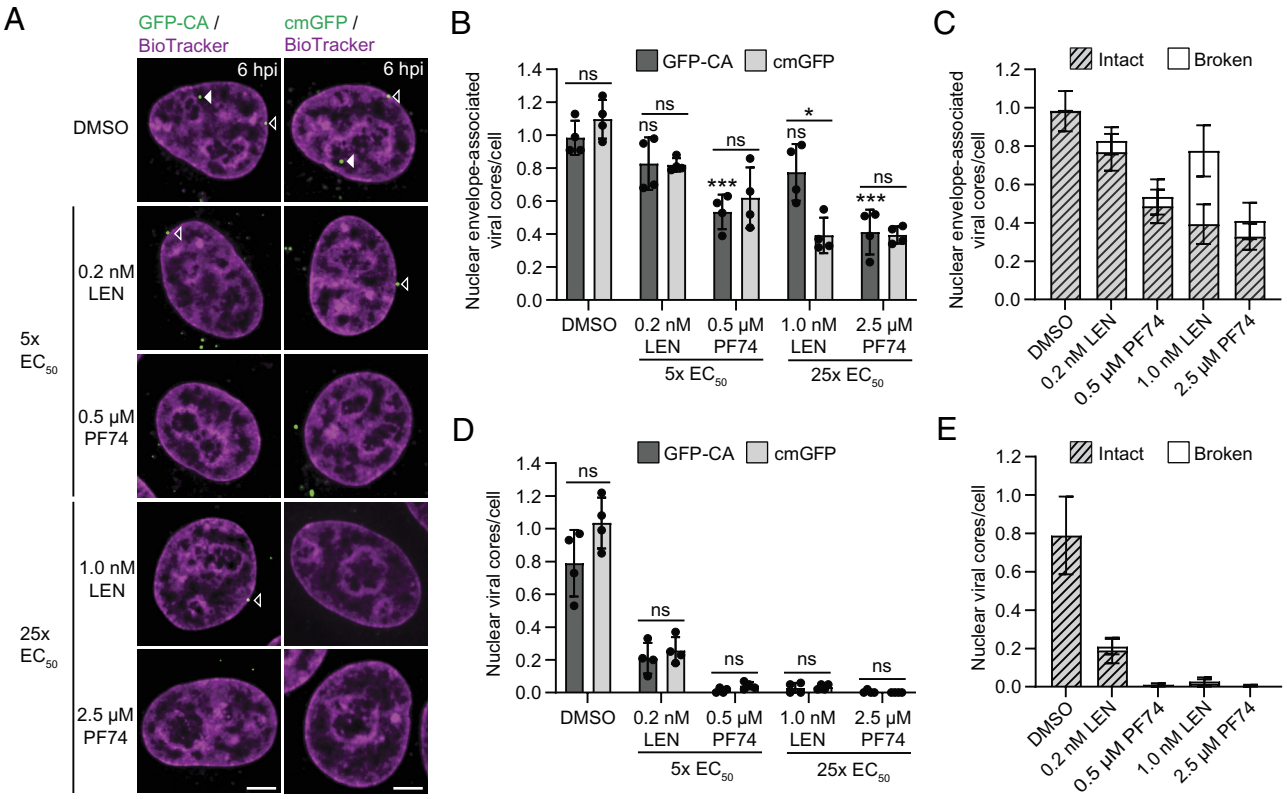

Fig. 7. Capsid inhibitors inhibit the nuclear import of viral cores by different mechanisms. (*A*) Representative images of nuclear envelope-associated (open triangle) and nuclear (filled triangle) HIV-1 cores labeled with GFP-CA (left column) or cmGFP (right column) in HeLa cells treated with equivalent effective concentrations (5× EC_{50} and 25× EC_{50}) of LEN and PF74 at the time of infection. Infected cells were stained with BioTracker 650 Red Nuclear Dye (magenta) and imaged by live-cell confocal microscopy approximately 6 h after infection. (Scale bar, 5 µm.) (*B*) Effect of capsid inhibitor treatment on the number of nuclear envelope-associated GFP-CA or cmGFP viral cores/cell. (*C*) Effect of capsid inhibitor treatment on the number of intact and broken viral cores associated with the nuclear envelope. The number of intact viral cores was determined by multiplying the number of GFP-CA viral cores/cell by the proportion of intact viral cores (number of cmGFP viral cores/cell ÷ GFP-CA viral cores/cell). The number of broken viral cores was determined by subtracting the number of intact viral cores/cell from the number of GFP-CA viral cores/cell. (*D*) Effect of capsid inhibitors on the number of nuclear GFP-CA or cmGFP viral cores/cell. (*E*) Effect of capsid inhibitor treatment on the number of intact and broken viral cores inside the nucleus. The number of nuclear viral cores that were intact or broken was calculated as in (*C*). For (*B*) and (*D*), an average of 64 cells in each independent experiment (ranging from 46 to 90) was analyzed for each condition; data are mean ± SD from four independent experiments. *P* values are from Welch's *t* test. ***$P < 0.001$; *$P < 0.05$; ns, not significant ($P > 0.05$).

0.2 nM LEN reduced nuclear import without disrupting viral cores, suggesting that LEN-induced changes to the capsid lattice can effectively inhibit viral core translocation into the nucleus. Interestingly, treatment with 1.0 nM LEN disrupted viral core integrity but did not reduce the viral core association with the nuclear envelope, indicating that broken cores can still dock at the nuclear envelope.

Discussion

In these studies, we employed two complementary viral core labeling techniques—GFP-CA for the capsid lattice and cmGFP for viral core integrity—to elucidate the effect of capsid inhibitor binding on HIV-1 capsids. Importantly, these labeling methods enabled us to determine the effects of LEN treatment on the HIV-1 capsid structure in infected cells, which has not been possible using previous methods. In vitro assays utilizing isolated HIV-1 cores indicated that LEN stabilizes the capsid lattice but simultaneously causes a loss of core integrity (Fig. 4*C*). These findings are consistent with previous studies using fate-of-capsid assays which showed that LEN increases the amount of pelletable capsid from cytoplasmic extracts (30, 31). Despite stabilization of the capsid lattice, we observed a ~3% and ~12% decrease in the median GFP-CA fluorescence intensity after treatment with 1 nM and 10 nM LEN (Fig. 4*D*), respectively, suggesting that a small portion of the capsid lattice is lost upon LEN binding, which likely results in loss of core integrity. In contrast, treatment with 10 µM PF74 resulted in a ~40% loss of detectable GFP-CA HIV-1 cores (Fig. 4*G*) and a ~34% decrease in the median GFP-CA fluorescence intensity of the remaining HIV-1 cores (Fig. 4*H*), indicating a substantial loss of the capsid lattice, which agrees with previous studies indicating that PF74 decreased the amount of pelletable capsid (16, 30, 34). Consistent with our fluorescence imaging data showing that PF74, but not LEN, leads to greater loss of the capsid lattice, we observed a higher percentage of capsids that had visible defects with 10 µM PF74 treatment (100X EC_{50}) compared to 10 nM LEN treatment (250X EC_{50}) (88% vs. 67%, respectively; $P < 0.0001$). These and other observations in our study show that PF74 and LEN utilize different mechanisms to inhibit HIV-1 replication.

Previous studies could not determine the integrity of the LEN-treated cores, whereas our fluorescence imaging experiments with purified capsids showed that treatment with 100 nM LEN resulted in loss of the cmGFP marker in nearly all capsids (Fig. 4*C*). Interestingly, in our electron microscopy experiments, 29% of the capsids treated with 100 nM LEN were classified as apparently intact, as no obvious holes were observed. These results suggest that nearly all the capsids classified as apparently intact after treatment with 100 nM LEN have small holes or ruptures that are not detectable by negative stain TEM. Similarly, some capsids classified as apparently intact after treatment with lower concentrations of LEN may have holes or ruptures that are not detectable. These

findings underscore the value of using cmGFP to assess viral core integrity in infected cells.

Treatment with 0.2 nM LEN (5X EC_{50}) inhibited nuclear import without disrupting core integrity, suggesting that LEN-induced changes in the capsid lattice without inducing capsid rupture are sufficient to inhibit nuclear import. These findings are consistent with a recent study showing that defects in nuclear import are associated with LEN-induced changes in viral core elasticity (46). Consistent with previous studies indicating that reverse transcription occurs within an intact capsid (9, 35), the decrease in reverse transcription products in cells treated with >1 nM LEN (23, 27) is likely due to the loss of core integrity, leading to dissociation of reverse transcriptase from the viral genome and degradation of the viral DNA by host nucleases (35). Sowd et al. showed that the antiviral activity of LEN and PF74 is increased in IP6-depleted cells (47), suggesting that the capsid stabilizing effect of IP6 antagonizes capsid inhibitors. IP6 was included in our in vitro experiments, and the cells used in the studies were capable of synthesizing IP6. It is possible that the concentrations at which LEN induces breaks in capsids may vary in different cells, depending on their endogenous IP6 concentrations.

A recent study by Faysal et al. (48) also utilized an in vitro, single-particle approach that simultaneously measured capsid content release and capsid lattice persistence (7) and concluded that LEN binding resulted in hyperstabilization of the capsid lattice and resultant loss of viral core integrity. In our studies, we were able to quantify the loss of core integrity and stabilization of the capsid lattice directly in infected cells and compare them to our in vitro studies using the same two methods to label viral cores. Our cell-based studies show that LEN treatment stabilizes the capsid lattice while inducing loss of core integrity (Fig. 4*C*). Our in vitro results and conclusions are in general agreement with those of Faysal et al. (48) with two notable differences. First, we directly measured capsid stability by determining the extent of loss of GFP-CA incorporated in the capsid lattice, whereas Faysal et al. indirectly measured capsid stability by monitoring the loss of fluorescently labeled CypA, a host protein that binds to and stabilizes HIV-1 capsids. The loss of CypA signal could have resulted from CypA dissociation rather than capsid lattice disassembly, as has been previously suggested for CypA-dsRED (33). Second, in the absence of drug treatment, Faysal et al. observed that most HIV-1 cores lost the GFP fluid phase marker and then rapidly (<2 min) lost most of the capsid lattice after viral membrane permeabilization. Both LEN (>50 nM) and PF74 (10 μM) accelerated the loss of HIV-1 core integrity whereas LEN was more effective than PF74 at preventing the loss of the capsid lattice typically observed in the no-drug control. In contrast, we observed that LEN stabilized broken HIV-1 capsids with minimal loss of the capsid lattice, whereas PF74 destabilized the broken HIV-1 capsids, resulting in significant loss of the capsid lattice.

We previously showed that intact HIV-1 cores enter the nucleus and uncoat near the integration site (4, 5). Our findings were primarily based on live-cell imaging of HIV-1 cores labeled with GFP-CA (4) or cmGFP (5). Here, we used in vitro immunofluorescence assays using isolated HIV-1 cores, anti-GFP(AF647) antibody, and cell-based MX2 restriction assays to establish that cmGFP is incorporated inside the HIV-1 capsids whereas GFP-CA is incorporated into the capsid lattice. These results disagree with the conclusions of a recent study by Francis et al. (36), which suggested that GFP-tagged CA was not incorporated into the mature capsid lattice but rather was incorporated into HIV-1 cores through direct interactions with the vRNP. These conclusions were largely based on the use of a mutant of cleavage and polyadenylation specificity factor 6 (CPSF6-358), which binds to cytoplasmic viral cores and inhibits infection (21). The authors reported that HIV-1 virions containing a mixture of the CPSF6-binding mutant N74D CA (~90%) and unlabeled WT CA (~10%), but not HIV-1 virions containing a mixture of N74D CA (~90%) and GFP-CA (~10%), were efficiently restricted by CPSF6-358. Based on this observation, it was concluded that the GFP-CA was inside the capsid since CPSF6-358 could not bind to these capsids and inhibit their infectivity. An alternative explanation, which the authors did not discuss, is that the GFP-CA fusion protein is incorporated into the capsid lattice, but the GFP that is displayed on the outside of the capsid interferes with CPSF6-358 binding to CA, similar to our observation that GFP-CA reduces sensitivity to MX2-mediated restriction. Additionally, our finding that GFP-CA in mature viral cores is accessible to the anti-GFP(AF647) antibody contradicts the view that it is not incorporated into the capsid lattice.

As we previously reported (4, 5), our viral core labeling methods had <2-fold effect on virus infectivity, enabling us to investigate the impact of capsid inhibitors on HIV-1 cores in infected cells by live-cell imaging. Consistent with our in vitro experiments with isolated HIV-1 cores, LEN treatment of infected cells resulted in the loss of integrity of all nuclear HIV-1 capsids. Additionally, our results that a significant proportion of LEN-treated cores disappear in infected cells (*SI Appendix*, Fig. S6) whereas they persist in vitro (Fig. 4*C*), suggest that binding of LEN and host factors to nuclear HIV-1 capsids destabilizes the capsid lattice, or that broken capsids are prone to disassembly or degradation by unidentified host mechanisms (49).

While PF74 is used exclusively in laboratory settings, LEN has received FDA approval for treating multidrug-resistant HIV-1 infection. Individuals receiving a single subcutaneous dose of LEN maintained a high plasma concentration (>10 nM; 250X EC_{50}) for nearly 6 mo (27). Clinical trials are in progress to evaluate the safety, pharmacokinetics, and efficacy of twice-yearly subcutaneous injections of LEN (https://www.clinicaltrials.gov). Our studies suggest that the plasma concentration of LEN will be sufficiently high to disrupt HIV-1 cores soon after the fusion of viral and host membranes, thereby preventing their nuclear import and leading to loss of virus infectivity. Interestingly, many broken viral cores could associate with the nuclear envelope, but only intact viral cores entered the nucleus. Although the mechanism of viral core translocation through nuclear pore complexes is not well understood, our data suggest that broken viral cores can associate with the nuclear pore complex, presumably through interactions between the capsid and nuclear pore proteins. However, essential steps required for nuclear entry do not occur after the stable docking of viral cores to nuclear pore complexes, perhaps due to changes in capsid elasticity (46). Overall, our results suggest that LEN prevents translocation of viral cores from the nuclear envelope to the nucleus, regardless of whether viral core integrity loss occurs. In contrast, PF74 treatment inhibits nuclear import by inhibiting the nuclear envelope docking of viral cores, highlighting their different mechanisms of nuclear import inhibition.

This study provides crucial insights into the mechanism of action of LEN in vitro and in vivo, a groundbreaking HIV-1 capsid inhibitor with potential to reshape HIV treatment strategies. By employing innovative capsid labeling techniques, we show that LEN uniquely disrupts the integrity of HIV-1 cores while simultaneously stabilizing the capsid lattice, thereby blocking the nuclear import of compromised viral cores. This dual action of LEN contrasts sharply with PF74, which destabilizes the capsid

lattice, leading to core disassembly. These findings underscore the therapeutic significance of LEN, particularly in combatting multidrug-resistant HIV-1 strains, by preventing the early stages of viral replication. This work not only deepens our understanding of capsid-targeting antivirals but also positions LEN as a vital tool in the ongoing fight against HIV, with implications for the development of next-generation therapies.

Materials and Methods

Experimental details and methods can be found in *SI Appendix*, including sources of cell lines and reagents, generation of HeLa:MX2 cell line, description of HIV-1-based vectors, and procedures for virus production and infection. Details of fractionation of HIV-1 cores using sucrose gradients, confocal microscopy of HIV-1 virions, mature HIV-1 cores, and immature HIV-1 particles in vitro, image processing and analysis, and negative stain electron microscopy of isolated HIV-1 cores are also described in *SI Appendix*. Live-cell confocal microscopy of HIV-1 cores in infected cells, and image processing and analysis are also described in *SI Appendix*.

Data, Materials, and Software Availability. All raw EM image files are available at Dryad (50). All other study data are included in the article and/or *SI Appendix*.

ACKNOWLEDGMENTS. The content of this publication does not necessarily reflect the views or policies of the Department of Health and Human Services, nor does mention of trade names, commercial products, or organizations imply endorsement by the US Government. This work was supported by the Intramural Research Program for the NIH, National Cancer Institute, Center for Cancer Research (Z1A BC011436 to V.K.P. and Z1A BC010504 to W.-S.H.) and supplemental funding provided by Office of AIDS Research (to V.K.P. and to W.-S.H.) to support collaborative interactions with the Behavior of HIV in Viral Environments Center (U54AI170855).

Author affiliations: [a]Viral Mutation Section, HIV Dynamics and Replication Program, Center for Cancer Research, National Cancer Institute at Frederick, Frederick, MD 21702; [b]Electron Microscopy Laboratory, Cancer Research Technology Program, Leidos Biomedical Research, Inc., Frederick National Laboratory for Cancer Research, Frederick, MD 21701; and [c]Viral Recombination Section, HIV Dynamics and Replication Program, Center for Cancer Research, National Cancer Institute at Frederick, Frederick, MD 21702

1. T. G. Muller, V. Zila, B. Muller, H. G. Krausslich, Nuclear capsid uncoating and reverse transcription of HIV-1. *Annu. Rev. Virol.* **9**, 261–284 (2022).
2. S. Mattei, B. Glass, W. J. Hagen, H. G. Krausslich, J. A. Briggs, The structure and flexibility of conical HIV-1 capsids determined within intact virions. *Science* **354**, 1434–1437 (2016).
3. O. Pornillos *et al.*, X-ray structures of the hexameric building block of the HIV capsid. *Cell* **137**, 1282–1292 (2009).
4. R. C. Burdick *et al.*, HIV-1 uncoats in the nucleus near sites of integration. *Proc. Natl. Acad. Sci. U.S.A.* **117**, 5486–5493 (2020).
5. C. Li, R. C. Burdick, K. Nagashima, W. S. Hu, V. K. Pathak, HIV-1 cores retain their integrity until minutes before uncoating in the nucleus. *Proc. Natl. Acad. Sci. U.S.A.* **118**, e2019467118 (2021).
6. J. I. Mamede, G. C. Cianci, M. R. Anderson, T. J. Hope, Early cytoplasmic uncoating is associated with infectivity of HIV-1. *Proc. Natl. Acad. Sci. U.S.A.* **114**, E7169–E7178 (2017).
7. C. L. Marquez *et al.*, Kinetics of HIV-1 capsid uncoating revealed by single-molecule analysis. *eLife* **7**, e34772 (2018).
8. A. Dharan, N. Bachmann, S. Talley, V. Zwikelmaier, E. M. Campbell, Nuclear pore blockade reveals that HIV-1 completes reverse transcription and uncoating in the nucleus. *Nat. Microbiol.* **5**, 1088–1095 (2020).
9. D. E. Christensen, B. K. Ganser-Pornillos, J. S. Johnson, O. Pornillos, W. I. Sundquist, Reconstitution and visualization of HIV-1 capsid-dependent replication and integration in vitro. *Science* **370**, eabc8420 (2020).
10. E. Rensen *et al.*, Clustering and reverse transcription of HIV-1 genomes in nuclear niches of macrophages. *EMBO J.* **40**, e105247 (2021).
11. A. Selyutina, M. Persaud, K. Lee, V. KewalRamani, F. Diaz-Griffero, Nuclear import of the HIV-1 core precedes reverse transcription and uncoating. *Cell Rep.* **32**, 108201 (2020).
12. T. G. Muller *et al.*, HIV-1 uncoating by release of viral cDNA from capsid-like structures in the nucleus of infected cells. *eLife* **10**, e64776 (2021).
13. S. Schifferdecker *et al.*, Direct capsid labeling of infectious HIV-1 by genetic code expansion allows detection of largely complete nuclear capsids and suggests nuclear entry of HIV-1 complexes via common routes. *mBio* **13**, e0195922 (2022).
14. V. Zila *et al.*, Cone-shaped HIV-1 capsids are transported through intact nuclear pores. *Cell* **184**, 1032–1046.e1018 (2021).
15. S. Bertagnolio *et al.*, Clinical impact of pretreatment human immunodeficiency virus drug resistance in people initiating nonnucleoside reverse transcriptase inhibitor-containing antiretroviral therapy: A systematic review and meta-analysis. *J. Infect Dis.* **224**, 377–388 (2021).
16. A. Bhattacharya *et al.*, Structural basis of HIV-1 capsid recognition by PF74 and CPSF6. *Proc. Natl. Acad. Sci. U.S.A.* **111**, 18625–18630 (2014).
17. W. S. Blair *et al.*, HIV capsid is a tractable target for small molecule therapeutic intervention. *PLoS Pathog.* **6**, e1001220 (2010).
18. T. Schaller *et al.*, HIV-1 capsid-cyclophilin interactions determine nuclear import pathway, integration targeting and replication efficiency. *PLoS Pathog.* **7**, e1002439 (2011).
19. R. C. Burdick, W. S. Hu, V. K. Pathak, Nuclear import of APOBEC3F-labeled HIV-1 preintegration complexes. *Proc. Natl. Acad. Sci. U.S.A.* **110**, E4780–4789 (2013).
20. F. Di Nunzio *et al.*, Human nucleoporins promote HIV-1 docking at the nuclear pore, nuclear import and integration. *PLoS ONE* **7**, e46037 (2012).
21. K. Lee *et al.*, Flexible use of nuclear import pathways by HIV-1. *Cell Host Microbe* **7**, 221–233 (2010).
22. K. A. Matreyek, A. Engelman, The requirement for nucleoporin NUP153 during human immunodeficiency virus type 1 infection is determined by the viral capsid. *J. Virol.* **85**, 7818–7827 (2011).
23. S. M. Bester *et al.*, Structural and mechanistic bases for a potent HIV-1 capsid inhibitor. *Science* **370**, 360–364 (2020).
24. Q. Shen *et al.*, The capsid lattice engages a bipartite NUP153 motif to mediate nuclear entry of HIV-1 cores. *Proc. Natl. Acad. Sci. U.S.A.* **120**, e2202815120 (2023).
25. S. Siddiqi, S. A. Siddiqi, C. M. Mansbach 2nd, Sec24C is required for docking the prechylomicron transport vesicle with the Golgi. *J. Lipid Res.* **51**, 1093–1100 (2010).
26. L. Wang *et al.*, Novel PF74-like small molecules targeting the HIV-1 capsid protein: Balance of potency and metabolic stability. *Acta Pharm. Sin. B* **11**, 810–822 (2021).
27. J. O. Link *et al.*, Clinical targeting of HIV capsid protein with a long-acting small molecule. *Nature* **584**, 614–618 (2020).
28. G. Wei *et al.*, Prion-like low complexity regions enable avid virus-host interactions during HIV-1 infection. *Nat. Commun.* **13**, 5879 (2022).
29. A. J. Price *et al.*, Host cofactors and pharmacologic ligands share an essential interface in HIV-1 capsid that is lost upon disassembly. *PLoS Pathog.* **10**, e1004459 (2014).
30. A. Selyutina *et al.*, GS-CA1 and lenacapavir stabilize the HIV-1 core and modulate the core interaction with cellular factors. *iScience* **25**, 103593 (2022).
31. J. E. Eschbach *et al.*, HIV-1 capsid stability and reverse transcription are finely balanced to minimize sensing of reverse transcription products via the cGAS-STING pathway. *mBio* **15**, e0034824 (2024).
32. A. C. Francis, M. Marin, J. Shi, C. Aiken, G. B. Melikyan, Time-resolved imaging of single HIV-1 uncoating in vitro and in living cells. *PLoS Pathog.* **12**, e1005709 (2016).
33. L. B. Gifford, G. B. Melikyan, HIV-1 capsid uncoating is a multistep process that proceeds through defect formation followed by disassembly of the capsid lattice. *ACS Nano* **18**, 2928–2947 (2024).
34. J. Shi, J. Zhou, V. B. Shah, C. Aiken, K. Whitby, Small-molecule inhibition of human immunodeficiency virus type 1 infection by virus capsid destabilization. *J. Virol.* **85**, 542–549 (2011).
35. R. C. Burdick *et al.*, HIV-1 uncoating requires long double-stranded reverse transcription products. *Sci. Adv.* **10**, eadn7033 (2024).
36. A. C. Francis *et al.*, Localization and functions of native and eGFP-tagged capsid proteins in HIV-1 particles. *PLoS Pathog.* **18**, e1010754 (2022).
37. J. A. Briggs *et al.*, The stoichiometry of Gag protein in HIV-1. *Nat. Struct. Mol. Biol.* **11**, 672–675 (2004).
38. S. Padilla-Parra *et al.*, Fusion of mature HIV-1 particles leads to complete release of a gag-GFP-based content marker and raises the intraviral pH. *PLoS ONE* **8**, e71002 (2013).
39. S. S. Smaga *et al.*, MxB restricts HIV-1 by targeting the tri-hexamer interface of the viral capsid. *Structure* **27**, 1234–1245.e1235 (2019).
40. C. Goujon *et al.*, Human MX2 is an interferon-induced post-entry inhibitor of HIV-1 infection. *Nature* **502**, 559–562 (2013).
41. M. Kane *et al.*, MX2 is an interferon-induced inhibitor of HIV-1 infection. *Nature* **502**, 563–566 (2013).
42. G. D. Moschonas *et al.*, MX2 forms nucleoporin-comprising cytoplasmic biomolecular condensates that lure viral capsids. *Cell Host Microbe* **32**, 1705–1724.e1714 (2024).
43. R. C. Burdick *et al.*, Dynamics and regulation of nuclear import and nuclear movements of HIV-1 complexes. *PLoS Pathog.* **13**, e1006570 (2017).
44. D. J. Wyma *et al.*, Coupling of human immunodeficiency virus type 1 fusion to virion maturation: A novel role of the gp41 cytoplasmic tail. *J. Virol.* **78**, 3429–3435 (2004).
45. D. McDonald *et al.*, Visualization of the intracellular behavior of HIV in living cells. *J. Cell Biol.* **159**, 441–452 (2002).
46. A. Deshpande *et al.*, Elasticity of the HIV-1 core facilitates nuclear entry and infection. *PLoS Pathog.* **20**, e1012537 (2024).
47. G. A. Sowd, J. Shi, C. Aiken, HIV-1 CA inhibitors are antagonized by inositol phosphate stabilization of the viral capsid in cells. *J. Virol.* **95**, e0144521 (2021).
48. K. M. R. Faysal *et al.*, Pharmacologic hyperstabilisation of the HIV-1 capsid lattice induces capsid failure. *eLife* **13**, e83605 (2024).
49. O. Schwartz, V. Marechal, B. Friguet, F. Arenzana-Seisdedos, J. M. Heard, Antiviral activity of the proteasome on incoming human immunodeficiency virus type 1. *J. Virol.* **72**, 3845–3850 (1998).
50. C. Li, R.-C. Hsia, R. Burdick, V. Pathak, Effect of Lenacapavir and PF74 on HIV-1 capsid morphology: EM images. Dryad. https://doi.org/10.5061/dryad.70rxwdc7z. Deposited 22 January 2025.